Dynamics of Continuous, Discrete and Impulsive Systems
Series **B:** *Applications & Algorithms* **19 (2012)** 411-430
 http://www.watsci.org

A FAMILY OF NOVEL CHAOTIC AND HYPERCHAOTIC ATTRACTORS FROM DELAY DIFFERENTIAL EQUATION

Hongtao Zhang[1], Xinzhi Liu[2*], Xuemin (Sherman) Shen[1], and Jun Liu [2]

[1] Department of Electrical and Computer Engineering,
University of Waterloo, Waterloo, Ontario N2L 3G1, Canada.
E-mails: h15zhang@gmail.com; xshen@bbcr.uwaterloo.ca.

[2] Department of Applied Mathematics,
University of Waterloo, Waterloo, Ontario N2L 3G1, Canada.
E-mails: xzliu@math.uwaterloo.ca; j49liu@math.uwaterloo.ca.

[*]Corresponding author. Phone: (519)888-4567 ext. 36007; Fax: (519)746-4319

Abstract. In this paper, a family of novel chaotic and hyperchaotic attractors are constructed utilizing a first-order delay differential equation (DDE). Dynamical analysis exhibits that Hopf bifurcation occurs at the non-trivial equilibrium points of the system when the time delay is properly selected. Bifurcation diagram and Lyapunov spectra further verify that the system behaves alternately in chaotic and periodic manners with the system parameter varying. By controlling the system parameter to increase the number of equilibrium points, a family of complex chaotic and hyper-chaotic attractors arise. Furthermore, we present a more general form of DDE and simulate its various chaotic dynamics under different-sign system parameters. The boundedness of this general DDE is studied in detail and finally, a possible circuit implement for these new attractors is proposed.

Keywords. Chaotic attractor, delay differential equation, Lyapunov exponent, Hopf bifurcation, chaos circuit.

1 Introduction

Chaos and hyperchaos have attracted a great deal of attention of scholars over the past two decades due to their potential applications to secure communication (see [1-8] and references therein). Chaotic signal with extreme sensitivity to initial conditions and noise-like dynamics is a natural carrier utilized to mask information in cryptography. Accordingly, how to construct appropriate chaotic or hyperchaotic systems becomes an active issue. Some typical multi-scroll attractors and hyperchaotic systems are presented in [9-17]. Also, the methods to generate chaos are more and more diversified. A non-autonomous technique to generate multi-scroll attractors and hyperchaos has been introduced [17-19]. Several switching methods to generate chaotic attractors have been achieved [17, 20-22]. Some fractional differential systems have been developed to generate chaos [13, 23-25]. In addition, some electronic circuits have been proposed to realize chaos [15, 17, 26-28].

DDE has been used to generate chaos since the discovery of Mackey-Glass system, a physiological model that exhibits chaotic behaviors. A few modified versions

have been reported [29-32], in which a piecewise nonlinearity is employed to substitude the original nonlinearity of Mackey-Glass system. Most recently, Yalçin and Özoguz [33] presented a new chaotic model in the following form:

$$\dot{x}(t) = a[-x(t-\tau) + \mathrm{sgn}(x(t-\tau))]$$

and, utilizing a hard limiter series, further generalized it to three-, four-, and five-scroll chaotic attractors. This system only possesses one positive Lyapunov exponent, not hyperchotic. Usually, in order to increase the complexity of the chaotic behavior, one needs to change the nonlinearity of the system and to make the system structure more complicated. Sprott [37] found the simplest DDE as follows:

$$\dot{x}(t) = \sin(x(t-\tau)).$$

When $7.8 < \tau \leq 40$, this system exhibits hyperchaotic behavior while it is unbounded. For application to secure communication, the chaotic carrier is required to be complex enough and bounded. Does there exist a simple DDE which is not only a multi-scroll attractor but also a bounded hyperchaos? How can one systematically increase the complexity of its chaotic dynamics while not making the system structure more complicated? Motivated by the above two systems, in this paper we present a new DDE which is bounded and can generate a family of novel chaotic and hyperchaotic attractors, called cell attractors. On keeping the system structure fixed, by system parameter control, one can obtain various hyperchaotic cell attractors with a desired number of positive Lyapunov exponents.

The remainder of this paper is organized as follows. In Section 2, we present a first-order DDE to generate new chaotic attractors and further generalize it to complex cell attractors by increasing its Hopf bifurcation points. In Section 3, a more general form of DDE is presented and a variety of novel chaotic dynamics are simulated under different-sign system parameters. In Section 4, The boundedness of the general DDE is studied and some boundedness conditions are obtained. In Section 5, a possible electronic circuit to realize these new attractors is proposed. Finally, some conclusions are given in Section 6.

2 New chaotic attractor

Consider the following DDE:

$$\dot{x}(t) = -ax(t-\tau) + b\sin(cx(t-\tau)), \tag{1}$$

where a, b, c, are constants, and τ is the time delay. For $a = 0.16$, $b = 0.4$, $c = 1.8$, and $\tau = 4.8$, Fig. 1(a) shows the trajectory portraits of $x(t)$ starting from two very close initial conditions and the error evolution $e(t) = x_1(t) - x_2(t)$ is shown in Fig. 1(b). It can be clearly observed that the dynamical behaviors become totally different after $t = 300s$, although the difference between the initial conditions (10^{-4}) is very tiny. This property is called the sensitivity to initial conditions, the unique characteristics of chaos. Fig. 2 shows the phase portrait of $x(t) - x(t-\tau)$.

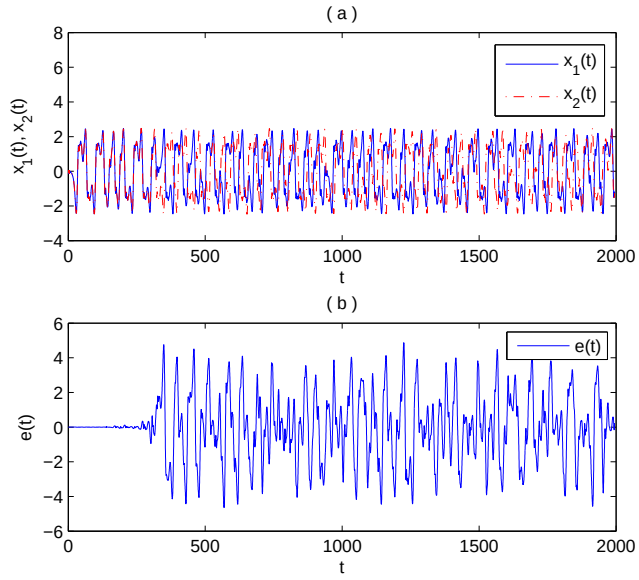

Figure 1: The state trajectories, $x_1(t)$ and x_2, starting from (a) $x_1(s) = 2\sin(6\pi(s+\tau))$ $(s \in [-\tau, 0])$ and (b) $x_2(s) = 2\sin(6\pi(s+\tau)) + 0.0001$ $(s \in [-\tau, 0])$, for $a = 0.16$, $b = 0.4$, $c = 1.8$, and $\tau = 4.8$.

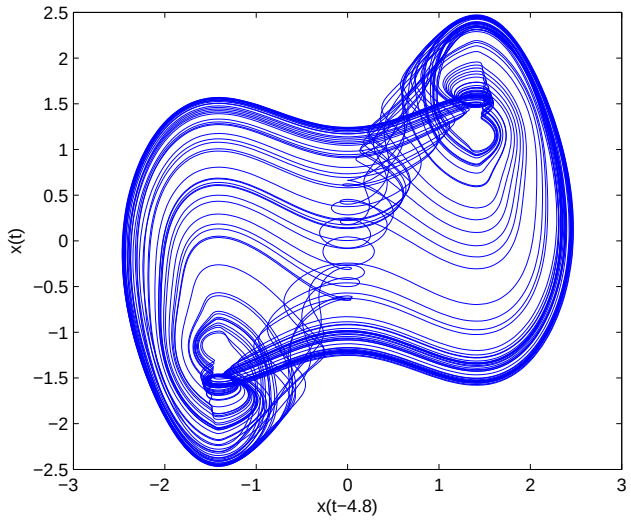

Figure 2: The phase portrait of $x(t-\tau) - x(t)$, when $a = 0.16$, $b = 0.4$, $c = 1.8$, and $\tau = 4.8$.

Furthermore, a variety of interesting dynamics of (1) can be obtained by varying the time delay alone. For $\tau = 4.98$, 5.3, 6, and 8, the phase portraits of $x(t) - x(t-\tau)$ are shown in Fig. 3.

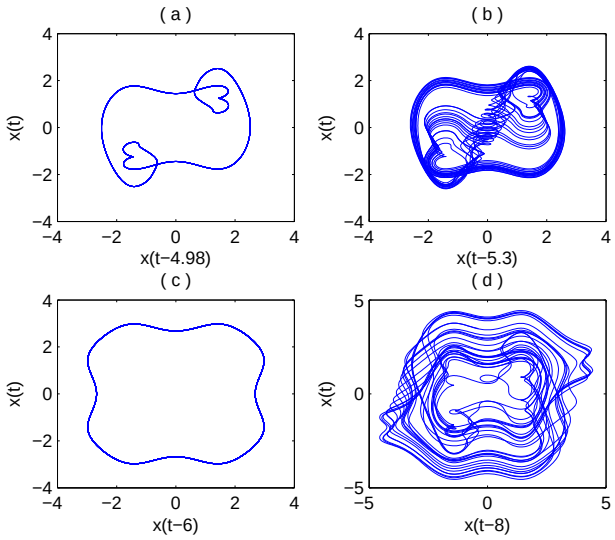

Figure 3: The phase portraits of $x(t-\tau) - x(t)$, when (a): $\tau = 4.98$, (b): $\tau = 5.3$, (c): $\tau = 6$, and (d): $\tau = 8$.

2.1 Dynamical analysis

For $a = 0.16$, $b = 0.4$, and $c = 1.8$, (1) has three equilibrium points $\{0, \pm 1.4119\}$. At each equilibrium point x^*, the characteristic equation of the corresponding linearization system is

$$\lambda + (a - bc\cos(cx^*))e^{-\lambda\tau} = 0. \tag{2}$$

In general, for DDE, there are no necessary and sufficient conditions known for all roots to be in the left half-plane. Here we study the stability and bifurcation of each equilibrium point by considering the scenario where a pair of complex conjugate roots cross the imaginary axis. For $x^* = \pm 1.4119$, the characteristic equation is

$$\lambda + 0.7542e^{-\lambda\tau} = 0. \tag{3}$$

Let $\lambda = u \pm vi$, $v \geq 0$. We have

$$\begin{cases} u + 0.7542e^{-u\tau}\cos(v\tau) = 0 \\ v - 0.7542e^{-u\tau}\sin(v\tau) = 0 \end{cases}$$

Differentiating both sides of the above equations with respect to τ gives

$$\begin{cases} \dot{u} - 0.7542e^{-u\tau}(\sin(v\tau)(\dot{v}\tau + v) + \cos(v\tau)(\dot{u}\tau + u)) = 0 \\ \dot{v} + 0.7542e^{-u\tau}(\sin(v\tau)(\dot{u}\tau + u) - \cos(v\tau)(\dot{v}\tau + v)) = 0 \end{cases}$$

When the roots cross the imaginary axis, their real parts equal to zero, i.e., $u = 0$. We have

$$\begin{cases} v = 0.7542 \\ \tau = 1.3259(\frac{\pi}{2} + 2k\pi), \quad k = 0, 1, ... \end{cases}$$

Thus,

$$\begin{cases} \frac{du}{d\tau}|_{\tau=2.0827} = 0.1640 \\ \frac{dv}{d\tau}|_{\tau=2.0827} = -0.2576 \end{cases}$$

Therefore, Hopf bifurcation occurs at $\tau = 2.0827$ where $k = 0$ since $\frac{du}{d\tau}|_{\tau=2.0827} \neq 0$ and the roots, other than $\pm 0.7542i$, all have negative real parts. It implies that for fixed parameters $a = 0.16$, $b = 0.4$, and $c = 1.8$, a pair of complex conjugate roots $\lambda_{1,2} = \pm 0.7542i$ cross the imaginary axis with τ varying around 2.0827. Thus, the equilibrium points $x^* = \pm 1.4119$ lose their stability and the solutions of (1) turn into a family of limit cycles.

For $x^* = 0$, the characteristic equation is

$$\lambda - 0.5600e^{-\lambda\tau} = 0. \tag{4}$$

Let $\lambda = vi$, $v \geq 0$. We have

$$\begin{cases} -0.5600\cos(v\tau) = 0 \\ v + 0.5600\sin(v\tau) = 0 \end{cases}$$

Thus,

$$\begin{cases} v = 0.5600 \\ \tau = 1.7857(\frac{3\pi}{2} + 2k\pi), \quad k = 0, 1, ... \end{cases}$$

At $\tau = 8.4149$ where $k = 0$, there exist a pair of complex conjugate roots $\pm 0.5600i$ cross the imaginary axis. However, there exists a root $\lambda = 0.1537$ lying in the right half-plane. Thus it is not a Hopf bifurcation here. This equilibrium point is unstable in the neighborhood of $\tau = 8.4149$.

Remark 1: By Hopf bifurcation we mean that an equilibrium point loses stability as a pair of complex conjugate eigenvalues of the linearization system around the equilibrium point cross the imaginary axis of the complex plane when suitable system parameters are given. This equilibrium point, which has lost its stability by Hopf bifurcation, is called a Hopf bifurcation point. We find that the appearance of Hopf bifurcation point is an important indication of chaos.

The roots of the characteristic equations at the equilibrium points $x^* = \pm 1.4119$ and $x^* = 0$ are shown in Fig. 4(a)-(b), respectively. It can be seen that Hopf bifurcations occur at $x^* = \pm 1.4119$ when $\tau = 2.0827$.

Furthermore, we calculate the maximal Lyapunov exponent $\lambda_{max} = 0.0211$ and Lyapunov dimension $d = 2.2718$ using the method in [35] and the Matlab LET toolbox. The Lyapunov spectra are shown in Fig. 5. The bifurcation diagrams vs the system parameters b and τ are shown in Fig. 6-7, respectively.

Remark 2: This chaotic system is sensitive to τ. Fig. 3 shows that when different time delays are chosen, (1) has different dynamic behaviors. Fig. 7 shows that the dynamics of (1) alternately switch between the chaotic and the periodic when τ

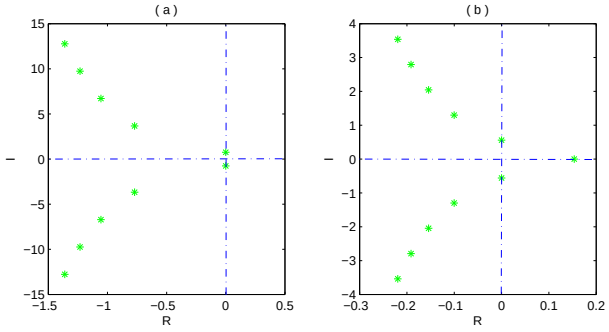

Figure 4: The roots of the characteristic equations of the corresponding linearization system of (1) at the equilibrium points (a) $x^* = \pm 1.4119$ when $\tau = 2.0827$ and (b) $x^* = 0$ when $\tau = 8.4149$.

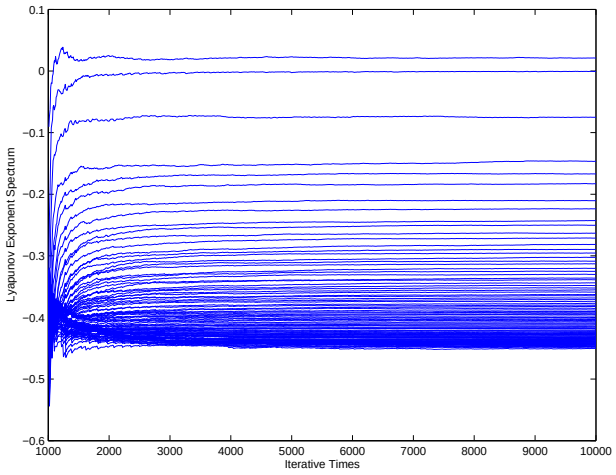

Figure 5: The Lyapunov spectra of (1) with $a = 0.16$, $b = 0.4$, $c = 1.8$ and $\tau = 4.8$.

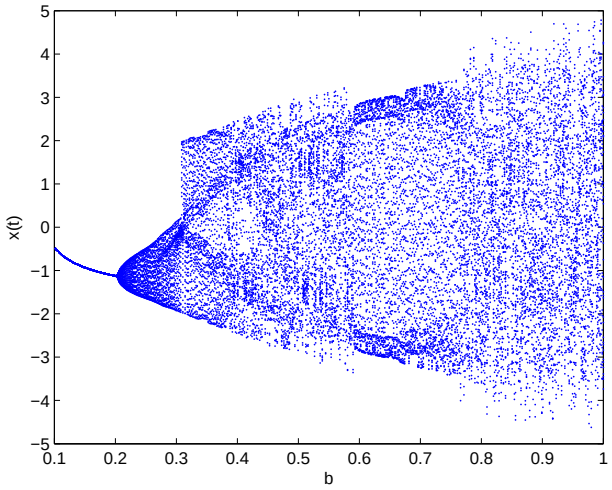

Figure 6: The bifurcation diagram vs b with $a = 0.16$, $c = 1.8$ and $\tau = 4.8$.

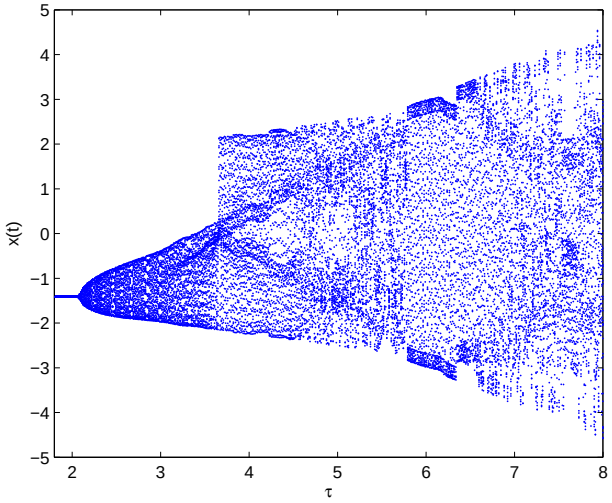

Figure 7: The bifurcation diagram vs τ with $a = 0.16$, $b = 0.4$ and $c = 1.8$.

varies in $[1.8,\ 8]$. Also, the dynamics of (1) is sensitive to the system parameter b. Fig. 6 shows that when b ranges in $[0.1,\ 1]$, the system alternately switch between the chaotic and the periodic.

2.2 Generalized hyperchaotic attractors

By increasing the number of Hopf bifurcation points, we can generalize (1) to more complex chaotic and hyperchaotic attractors.

When $a = 0.16$, $b = 0.8$, and $c = 1.8$, (1) has seven equilibrium points (0, ± 1.5681, ± 4.0071, ± 4.5899). Hopf bifurcation occurs at points (± 1.5681, ± 4.5899). Fig. 8 shows that (1) can achieve more complex cell chaos when τ increases. When $\tau = 4.0$, the system has only one positive Lyapunov exponent $\lambda = 0.0493$ and Lyapunov dimension $d = 3.1035$. When $\tau = 8.0$, the system has two positive Lyapunov exponents $\lambda_1 = 0.0718$, $\lambda_2 = 0.0189$ and Lyapunov dimension $d = 5.0807$. Here the system becomes a hyperchaos, which possesses more than one positive Lyapunov exponents.

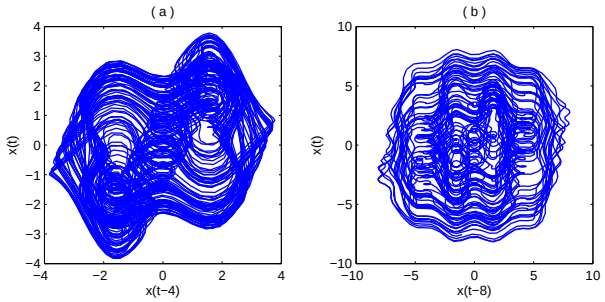

Figure 8: The phase portraits of $x(t-\tau)-x(t)$ with $b = 0.8$, when (a): $\tau = 4$ and (b): $\tau = 8$.

When $a = 0.16$, $b = 1.6$, and $c = 1.8$, (1) has eleven equilibrium points (0, ± 1.6531, ± 3.7013, ± 4.9484, ± 7.4481, ± 8.1932). Hopf bifurcation occurs at points (± 1.6531, ± 4.9484, ± 8.1932). The phase portraits of $x(t)-x(t-\tau)$ are shown in Fig. 9. When $\tau = 2.5$, the system has only one positive Lyapunov exponent $\lambda = 0.0627$ and Lyapunov dimension $d = 3.5655$. When $\tau = 4.0$, the system has two positive Lyapunov exponents $\lambda_1 = 0.0795$, $\lambda_2 = 0.0319$ and Lyapunov dimension $d = 5.4147$. When $\tau = 6.0$, the system has three positive Lyapunov exponents $\lambda_1 = 0.0912$, $\lambda_2 = 0.0630$, $\lambda_3 = 0.0156$ and Lyapunov dimension $d = 7.8406$. When $\tau = 8.0$, the system has four positive Lyapunov exponents $\lambda_1 = 0.1061$, $\lambda_2 = 0.0705$, $\lambda_3 = 0.0339$, $\lambda_4 = 0.0078$ and Lyapunov dimension $d = 10.0316$. With τ increasing, the system also turns into a hyperchaos.

When $a = 0.16$, $b = 2.4$, and $c = 1.8$, (1) has fourteen equilibrium points (0, ± 1.6786, ± 3.6366, ± 5.0317, ± 7.2854, ± 8.3706, ± 10.9723, ± 11.6698). Hopf bifurcation occurs at points (± 1.6786, ± 5.0317, ± 8.3706, ± 11.6698). The phase portraits of $x(t)-x(t-\tau)$ are shown in Fig. 10. When $\tau = 1.5$, the system has

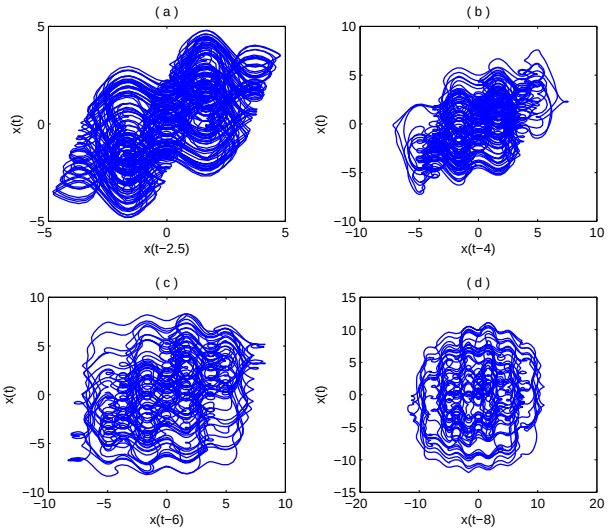

Figure 9: The phase portraits of $x(t-\tau)-x(t)$ with $b=1.6$, when (a): $\tau=2.5$, (b): $\tau=4$, (c): $\tau=6$, and (d): $\tau=8$.

only one positive Lyapunov exponent $\lambda=0.0577$ and Lyapunov dimension $d=3.2522$. When $\tau=3.0$, the system has two positive Lyapunov exponents $\lambda_1=0.0807$, $\lambda_2=0.0422$ and Lyapunov dimension $d=6.0047$. When $\tau=4.0$, the system has three positive Lyapunov exponents $\lambda_1=0.0925$, $\lambda_2=0.0593$, $\lambda_3=0.0259$ and Lyapunov dimension $d=7.8487$. When $\tau=5.0$, the system has four positive Lyapunov exponents $\lambda_1=0.1042$, $\lambda_2=0.0685$, $\lambda_3=0.0151$, $\lambda_4=0.0685$ and Lyapunov dimension $d=9.6047$. When $\tau=6.0$, the system has five positive Lyapunov exponents $\lambda_0.1086$, $\lambda_2=0.0786$, $\lambda_3=0.0498$, $\lambda_4=0.0262$, $\lambda_5=0.0046$ and Lyapunov dimension $d=11.4108$. When $\tau=8.0$, the system has six positive Lyapunov exponents $\lambda_1=0.1210$, $\lambda_2=0.0927$, $\lambda_3=0.0634$, $\lambda_4=0.0410$, $\lambda_5=0.0191$, $\lambda_6=0.0067$ and Lyapunov dimension $d=14.8941$. With τ increasing, it also turns into a hyperchaos.

By further increasing b, we can increase the number of equilibrium points and that of Hopf bifurcation points of (1). Accordingly, the number of positive Lyapunov exponents and Lyapunov dimension increase and the system turns into more complex hyperchaotic attractors. Fig. 11 shows that the maximum 10 lyapunov exponents evolve as b varies in $[0.1,\ 3]$ for fixed parameters $a=0.16$, $c=1.8$ and $\tau=8.0$.

Remark 3: We find that the number of Hopf bifurcation points has a close relation with the complexity of the new chaotic attractors. By increasing b, we can increase the number of Hopf bifurcation points of (1). Furthermore, we can obtain more complex chaos with more positive Lyapunov exponents and higher Lyapunov

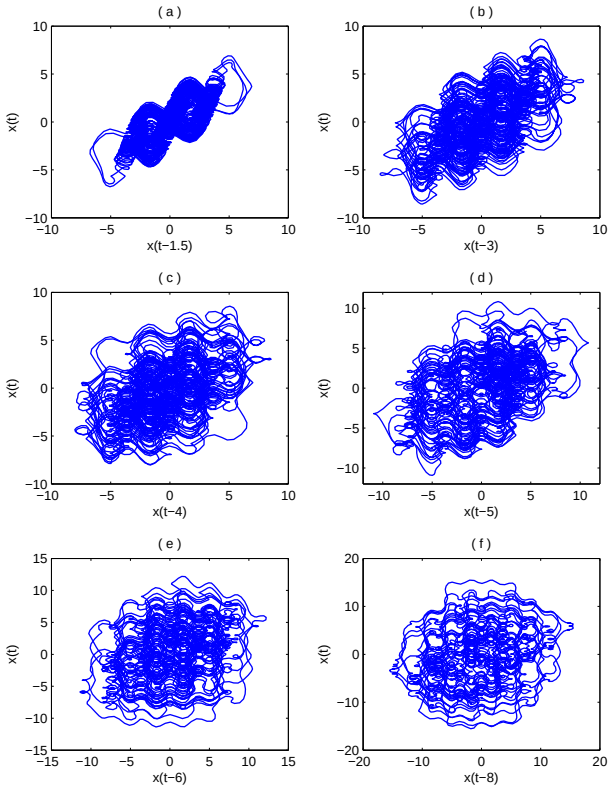

Figure 10: The phase portraits of $x(t-\tau)-x(t)$ with $b=2.4$, when (a): $\tau=1.5$, (b): $\tau=3$, (c): $\tau=4$, (d): $\tau=5$, (e): $\tau=6$, and (f): $\tau=8$.

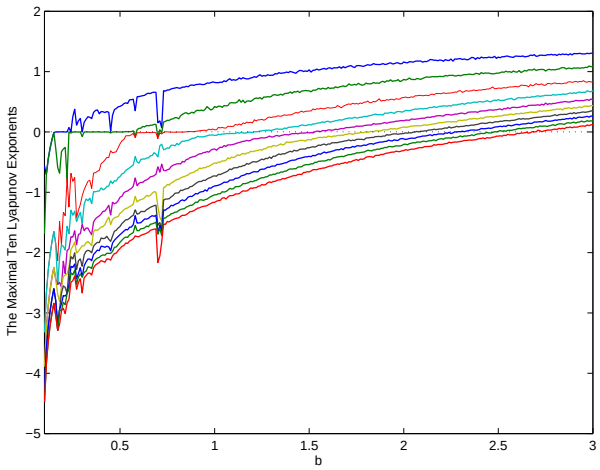

Figure 11: The maximum ten Lyapunov exponents vs b in $[0.1,3]$ with $a = 0.16$, $c = 1.8$ and $\tau = 8.0$.

dimension.

3 General DDE generating chaos

In this section, we present a more general model to generate chaos. Consider the following DDE:

$$\dot{x}(t) = a_1 x(t) + a_2 x(t-\tau_1) + b\sin(cx(t-\tau_2)), \tag{5}$$

where a_1, a_2, b, c, are constants, and $\tau_1, \tau_2, (\tau_1 > 0,\ \tau_2 > 0)$ are the time delays.

3.1 Special case I: Ikeda Equation

Let $a_1 = -0.32$, $a_2 = 0$, $b = 1$, and $c = 1.8$, (5) transforms to the Ikeda equation. Fig. 12 shows its phase portraits of $x(t)$-$x(t-\tau_2)$ with different values of τ_2, which are similar to that in [34].

3.2 Special case II

Let $a_1 = 0$, $a_2 = -0.24$, $b = 0.5$, $c = 1.8$, $\tau_1 = 4$, and $\tau_2 = 6$. (5) generates chaotic behavior. Fig. 13 shows its phase portraits of $x(t)$-$x(t-\tau_1)$-$x(t-\tau_2)$ when suitable time delays are selected.

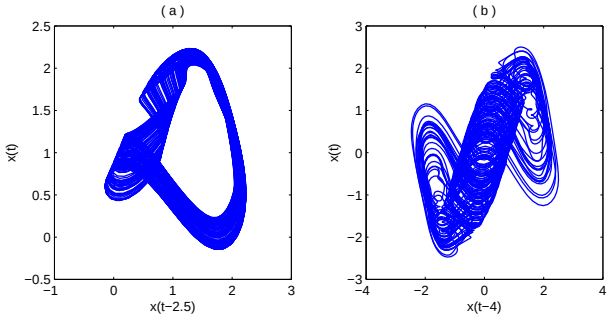

Figure 12: The phase portraits of $x(t)$-$x(t-\tau_2)$, when (a): $\tau_2 = 2.5$ and (b): $\tau_2 = 4$.

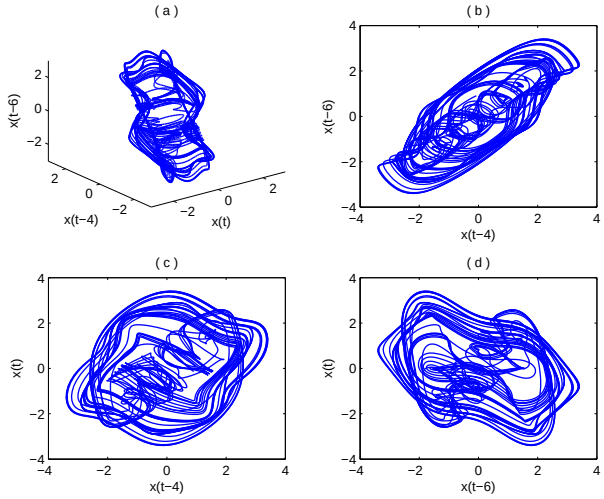

Figure 13: The phase portraits of $x(t)$-$x(t-\tau_1)$-$x(t-\tau_2)$, when $\tau_1 = 4$ and $\tau_2 = 6$.

3.3 Special case III

Let $a_1 = -0.08$, $a_2 = -0.08$, $b = 0.5$, and $c = 1.8$. (5) generates chaotic behavior. Fig.14 shows its phase portraits of $x(t)$-$x(t-\tau_1)$-$x(t-\tau_2)$ when suitable time delays are selected.

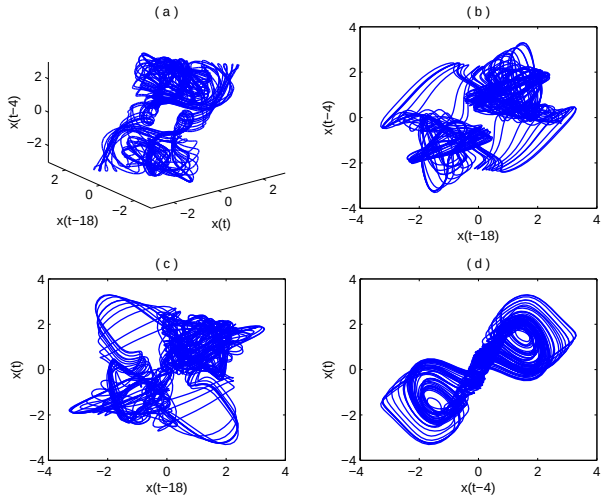

Figure 14: The phase portraits of $x(t)$-$x(t-\tau_1)$-$x(t-\tau_2)$, when $\tau_1 = 18$ and $\tau_2 = 4$.

3.4 Special case IV

Let $a_1 = -0.08$, $a_2 = 0.08$, $b = 0.5$, and $c = 1.8$. (5) generates chaotic behavior. Fig.15 shows its phase portraits of $x(t)$-$x(t-\tau_1)$-$x(t-\tau_2)$ when suitable time delays are selected.

3.5 Special case V

Let $a_1 = 0.32$, $a_2 = -0.48$, $b = 0.5$, and $c = 1.8$. (5) generates chaotic behavior. Fig.16 shows its phase portraits of $x(t)$-$x(t-\tau_1)$-$x(t-\tau_2)$ when suitable time delays are selected.

Remark 4: Because of the different signs of a_1 and a_2, special cases I-V exhibit different dynamical behaviors. And all these special cases can generate more complex chaotic attractors by increasing the number of Hopf bifurcation points of (5).

4 Boundedness analysis

In general, a system is said to be chaotic if it possesses one positive Lyapunov exponent and is bounded. Numerical computation has shown that all above attractors

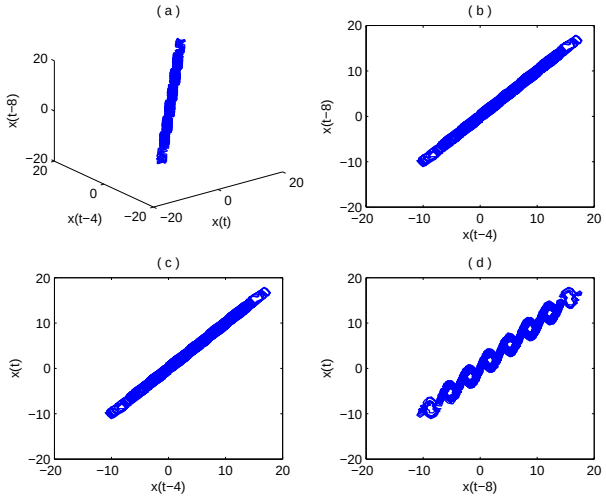

Figure 15: The phase portraits of $x(t)$-$x(t-\tau_1)$-$x(t-\tau_2)$, when $\tau_1 = 1$ and $\tau_2 = 10$.

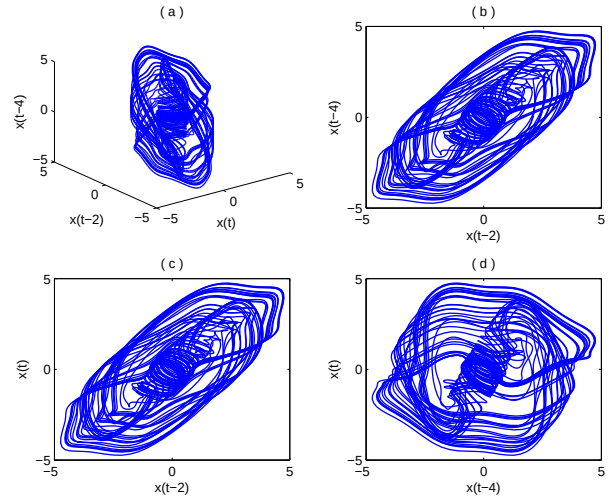

Figure 16: The phase portraits of $x(t)$-$x(t-\tau_1)$-$x(t-\tau_2)$, when $\tau_1 = 2$ and $\tau_2 = 4$.

have at least one positive Lyapunov exponent. In this section, we will study the boundedness of (5) and obtain its boundedness conditions. Consider the following general DDE:

$$\dot{x}(t) = Ax(t) + Bx(t-r) + f(x(t), x(t-r)), \tag{6}$$

where A, B and r are constants with $r > 0$, f is a nonlinear perturbation, and x is scalar. Without the perturbation, (6) reduces to the linear homogeneous DDE,

$$\dot{x}(t) = Ax(t) + Bx(t-r). \tag{7}$$

Lemma 1: Suppose that the function f is locally Lipchitz in both variables. Then the solution $x(t) = x(t,\phi)$ of (6) with initial data $x(t) = \phi(t)$ on $[-r, 0]$ is given by

$$x(t) = y(t) + \int_0^t X(t-s) f(x(s), x(s-r)) ds, \tag{8}$$

where $y(t) = y(t,\phi)$ is the solution of the homogeneous equation (7) with initial data $y(t) = \phi(t)$ on $[-r, 0]$ and X is the fundamental solution of (7), i.e., the solution of (7) with initial data

$$\psi(t) = \begin{cases} 0, & -r \le t < 0, \\ 1, & t = 0. \end{cases}$$

Proof: By (8), we see that $x(t) = y(t) = \phi(t)$ on $[-r, 0]$. By uniqueness, it suffices to show that $x(t)$ given by (8) satisfies (6). In fact, by (8), we have

$$\begin{aligned}
& \dot{x}(t) \\
= \; & \dot{y}(t) + f(x(t), x(t-r)) + \int_0^t \dot{X}(t-s) f(x(s), x(s-r)) ds \\
= \; & Ay(t) + By(t-r) + f(x(t), x(t-r)) \\
& + \int_0^t [AX(t-s) + BX(t-s-r)] f(x(s), x(s-r)) ds \\
= \; & A[y(t) + \int_0^t X(t-s) f(x(s), x(s-r)) ds] \\
& + B[y(t-r) + \int_0^{t-r} X(t-s-r) f(x(s), x(s-r)) ds] \\
= \; & Ax(t) + Bx(t-r) + f(x(t), x(t-r)),
\end{aligned}$$

where $X(t-s-r) \equiv 0$ for $s \in (t-r, \quad t]$ is used. The proof is complete.

Define the characteristic equation of system (7) as follows,

$$h(\lambda) \stackrel{def}{=} \lambda - A - Be^{-\lambda r}. \tag{9}$$

Let $Re(\lambda)$ designate the real part of λ.

Lemma 2: For the homogeneous equation (7), if $\varepsilon_0 = \max\{Re(\lambda) : h(\lambda) = 0\}$, then, for any $\varepsilon_1 > \varepsilon_0$, there is a constant $k_1 = k_1(\varepsilon_1)$ such that the fundamental solution $X(t)$ satisfies the inequality

$$|X(t)| \leq k_1 e^{\varepsilon_1 t}, \qquad t \geq 0. \tag{10}$$

The detailed proof can be found in ***Theorem 5.2*** of Chapter 1 in [36].

Lemma 3: Suppose $\varepsilon_0 = \max\{Re(\lambda) : h(\lambda) = 0\}$ and $x(t) = x(t, \phi)$ is the solution of the homogeneous equation (7), which coincides with ϕ on the $[-r, 0]$. Then, for any $\varepsilon_2 > \varepsilon_0$, there is a constant $k_2 = k_2(\varepsilon_2, \phi)$ such that

$$|x(t)| \leq k_2 e^{\varepsilon_2 t}, \qquad t \geq 0. \tag{11}$$

The detailed proof can be found in ***Theorem 6.2*** of Chapter 1 in [36].

Lemma 4: All roots of the equation $(z+a)e^z + b = 0$, where a and b are real, have negative real parts if and only if

$$a > -1$$
$$a + b > 0$$
$$b < \zeta \sin\zeta - a\cos\zeta$$

where ζ is the root of $\zeta = -a\tan\zeta$, $0 < \zeta < \pi$, if $a \neq 0$ and $\zeta = \pi/2$ if $a = 0$.

The detailed proof can be found in ***Theorem A.5*** of Appendix in [36].

Theorem 1: For system (6), if the nonlinear perturbation is locally Lipschitz in both variables, bounded, i.e., $|f| \leq M (M > 0)$, and

$$Ar < 1, \tag{12}$$
$$A + B < 0, \tag{13}$$
$$-Br < \zeta \sin\zeta + Ar\cos\zeta. \tag{14}$$

where ζ is the root of $\zeta = Ar\tan\zeta$, $0 < \zeta < \pi$, if $A \neq 0$ and $\zeta = \pi/2$ if $A = 0$, then the solutions of system (6) are bounded.

Proof: By inequalities (11), (12), (13) and ***Lemma 4***, all roots of the characteristic equation $\lambda - A - Be^{-\lambda r} = 0$ have negative real parts. So the conditions of ***Lemmas*** 2 and 3 are satisfied. Then, we have

$$|y(t)| \leq k_1 e^{\varepsilon_1 t}, \quad |X(t)| \leq k_2 e^{\varepsilon_2 t}, \quad t \geq 0. \tag{15}$$

where k_1 and k_2 are positive constants, ε_1 and ε_2 are negative constants, $y(t)$ is the solution of (7) with the initial value ϕ and $X(t)$ is the fundamental solution of (7).

Let $x(t)$ be the solution of (6). By ***Lemma*** 1, we obtain

$$\begin{aligned} |x(t)| &\leq |y(t)| + M\int_0^t |X(t-s)|ds \\ &\leq k_1 e^{\varepsilon_1 t} + Mk_2\int_0^t e^{\varepsilon_2(t-s)}ds \\ &\leq k_1 e^{\varepsilon_1 t} + \frac{Mk_2}{\varepsilon_2}(e^{\varepsilon_2 t}-1) \\ &\leq k_1, \qquad t \geq 0. \end{aligned}$$

The proof is complete.

By letting $A = 0$, $B = -ab$ and $r = \tau$ in (6), we have the following result.

Corollary 1: The solutions of system (1) are bounded, for arbitrary c and d, provided that

$$0 < ab\tau < \pi/2. \tag{16}$$

Corollary 2: The solutions of system 5 are bounded, for arbitrary c, d and τ_2, provided that

$$ab_0\tau_1 < 1, \tag{17}$$

$$ab_0 + ab_1 < 0, \tag{18}$$

$$-ab_1\tau_1 < \zeta\sin\zeta + ab_0\tau_1\cos\zeta. \tag{19}$$

where ζ is the root of $\zeta = ab_0\tau_1\tan\zeta$, $0 < \zeta < \pi$, if $ab_0 \neq 0$ and $\zeta = \pi/2$ if $ab_0 = 0$.
Proof: It follows from ***Theorem 1*** by letting $A = ab_0$, $B = ab_1$ and $r = \tau_1$.
Corollary 3: If $b_1 = 0$, the solutions of system (5) which turns into the famous Ikeda Equation are bounded, for arbitrary c and d, provided that

$$ab_0 < 0. \tag{20}$$

Proof: It follows from ***Corollary 2*** with $b_1 = 0$. Actually, condition (20) implies conditions (17) and (18) when $b_1 = 0$. Moreover, $ab_0 < 0$ implies $\zeta \in (\frac{\pi}{2}, \pi)$, and then condition (19) is always satisfied as

$$\begin{aligned} \zeta\sin\zeta + ab_0\tau_1\cos\zeta &= \frac{ab_0\tau_1\sin^2\zeta + ab_0\tau_1\cos^2\zeta}{\cos\zeta} \\ &= \frac{ab_0\tau_1}{\cos\zeta} > 0, \quad \zeta \in (\frac{\pi}{2}, \pi). \end{aligned}$$

5 Circuit implement

A possible electronic circuit to realize (1) is shown in Fig. 17. This circuit mainly consists of a tunable delay unit, a sine function, three gain controllers and an integrating circuit, which comprises resistors, capacitors and op-amps.

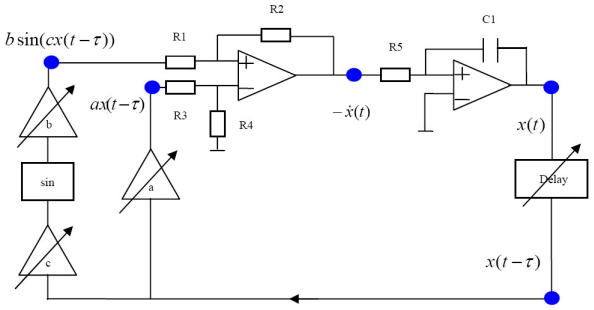

Figure 17: The electronic circuit to realize the new attractors.

The tunable delay unit employed here can be realized using an artificial delay line [30]. A commercial trigonometric function chip AD639 is chosen to work as sine function whose details can be found in [38-39]. Three gain controllers are designed to control the corresponding system parameters a, b, c, respectively, as shown in Fig. 18.

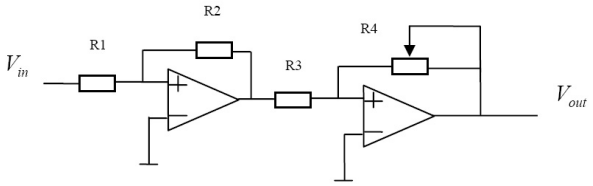

Figure 18: Circuit for gain controllers.

6 Conclusion

We have constructed a family of novel chaotic and hyperchaotic attractors from DDE and analyzed their chaotic dynamics. A systematical method to generalize the new chaotic system to complex chaotic and hyperchaotic attractors has been developed. Furthermore, a general DDE has been discussed and various chaotic behaviors have been simulated under different-sign system parameters. Boundedness of solutions has been studied and some sufficient conditions for boundedness have been obtained. Finally, a possible circuit framework is designed to realize these new attractors. To further develop its application to secure communication in reality, there is an outstanding issue needed to be solved in an urgent manner, synchronization of new chaotic systems. In future work, we will study its synchronization criteria and explore various feasible secure communication schemes based on it.

References

[1] L.M. Pecora and T.L. Carroll, Synchronization in chaotic systems, *Phys. Rev. Lett.*, **64**, (1990) 821-824.

[2] K.M. Cuomo and A.V. Oppenheim, Circuit implementation of synchronized chaos with applications to communications, *Phys. Rev. Lett.*, **71**, (1993) 65-68.

[3] G. Grassi and S. Mascolo, A system theory approach for designing cryptosystems based on hyperchaos, *IEEE Trans. Circuits Syst., I*, **46**, (1999) 1135-1138.

[4] K.S. Halle, C.W. Wu, M. Itoh, and L.O. Chua, Spread spectrum communication through modulation of chaos, *Int. J. Bifur. Chaos*, **3**, (1993) 469-477.

[5] T. Yang and L.O. Chua, Impulsive stabilization for control and synchronization of chaotic systems: Theory and application to secure communication, *IEEE Trans. Circuits Syst., I*, **44**, (1997) 976-988.

[6] J. Goedgebuer, L. Larger, and H. Porte, Optical cryptosystem based on synchronization of hyperchaos generated by a delayed Feedback tunable laser diode, *Phys. Rev. Lett.*, **80**, (1998) 2249-2252.

[7] H. Dimassi and A. Loría, Adaptive unknown-input observers-based synchronization of chaotic systems for telecommunication, *IEEE Trans. Circuits Syst., I*, **58**, (2011) 800-812.

[8] X. Liu, X. Shen, and H.T. Zhang, Intermittent impulsive synchronization of chaotic delayed neural networks, *Differential Equations and Dynamical Systems*, **19**, (2011) 149-169.

[9] O.E. Rossler, An equation for hyperchaos, *Phys. Lett. A*, **71**, (1979) 155-157.

[10] J. Goedgebuer, L. Larger, and H. Porte, Optical cryptosystem based on synchronization of hyperchaos generated by a delayed Feedback tunable laser diode, *Phys. Rev. Lett.*, **80**, (1998) 2249-1152.

[11] G. Grassi and S. Mascolo, Synchronizing hyperchaotic systems by observer design, *IEEE Trans. Circuits Syst., II*, **46**, (1999) 478-483.

[12] X. Liu, X. Shen, and H.T. Zhang, Multi-scroll chaotic and hyperchaotic attractors generated from Chen system, *Int. J. Bifurc. Chaos*, **22**, (2012) 1250033.

[13] C. Li and G. Chen, Chaos and hyperchaos in the fractional-order Rossler equations, *Physica A*, **341**, (2004) 55-61.

[14] Y. Li, W. Tang, and G. Chen, Generating hyperchaos via state feedback control, *Int. J. Bifurc. Chaos*, **15**, (2005) 3367-3375.

[15] M.E. Yalcin, Multi-scroll and hypercube attractors from a general jerk circuit using Josephson junctions, *Chaos, Soliton & Fractals*, **34**, (2007) 1659-1666.

[16] Z.Y. Yan and P. Yu, Hyperchaos synchronization and control on a new hyperchaotic attractor, *Chaos, Soliton & Fractals*, **35**, (2008) 333-345.

[17] J. Lu, F. Han, X. Yu, and G. Chen, Generating 3-D multi-scroll chaotic attractors: a hysteresis series switching method, *Automatica*, **40**, (2004) 1677-1687.

[18] A.S. Elwakil and S. Ozoguz, Multi-scroll chaotic oscillators: the nonautonomous approach, *IEEE Trans. Circuits Syst., II*, **53**, (2006) 862-866.

[19] Y. Li, X. Liu, and H.T. Zhang, Dynamical analysis and impulsive control of a new hyperchaotic system, *Mathematical and Computer Modelling*, **42**, (2005) 1359-1374.

[20] J. Lu and G. Chen, Generating multiscroll chaotic attractors: theories, methods and applications, *Int. J. of Bifurcation and Chaos*, **16**, (2006) 775-858.

[21] J. Lu, G. Chen, X. Yu, and H. Leung, Design and analysis of multi-scroll chaotic attractors from saturated function series, *IEEE Trans. Circuits Syst. I*, **51**, (2004) 2476-2490.

[22] X. Liu, K.L. Teo, H.T. Zhang, and G. Chen, Switching control of linear systems for generating chaos, *Chaos, Solitons & Fractals*, **30**, (2006) 725-733.

[23] T. Hartley, C. Lorenzo, and H.K. Qammer, Chaos in a fractional order Chua's system, *IEEE Trans. Circuits Syst., I*, **42**, (1995) 485-490.

[24] W.M. Ahmad and J.C. Sprott, Chaos in fractional-order autonomous nonlinear systems, *Chaos, Solitons & Fractals*, **16**, (2003) 339-351.

[25] C. Li and G. Chen, Chaos in the fractional order Chen system and its control, *Chaos, Solitons & Fractals*, **22**, (2004) 549-554.

[26] L.O. Chua, C.W. Wu, A. Huang, and G. Zhong, A universal circuit for studying and generating chaos, I. Routes to chaos, *IEEE Trans. Circuits Syst., I*, **40**, (1993) 732-744.

[27] M. Yalcin, J. Suykens, J. Vandewalle, and S. Ozoguz, Families of scroll grid attractors, *Int. J. Bifurc. Chaos*, **12**, (2002) 23-41.

[28] A.S. Elwakil and M.P. Kennedy, Construction of classes of circuit-independent chaotic oscillator-susing passive-only nonlinear devices, *IEEE Trans. Circuits Syst., I*, **48**, (2001) 289-307.

[29] H. Lu and Z. He, Chaotic behavior in first-order autonomous continuous-time systems with delay, *IEEE Trans. Circuits Syst., I*, **43**, (1996) 700-702.

[30] A. Namajunas, K. Pyragas, and A. Tamasevicius, An electronic analog of the Mackey-Glass system, *Phys. Lett. A*, **201**, (1995) 42-46.

[31] A. Tamasevicius, G. Mykolaitis, and S. Bumeliene, Delayed feedback chaotic oscillator with improved spectral characteristics, *Electron. Lett.*, **42**, (2006) 736-737.

[32] L. Wang, X. Yang, J. Vandewalle, and S. Ozoguz, Generation of multi-scroll delayed chaotic oscillator, *Electron. Lett.*, **42**, (2006) 1439-1441.

[33] M. Yalcin and S. Ozoguz, N-scroll chaotic attractors from a first-order time-delay differential equation, *Chaos*, **17**, (2007) 033112.

[34] K. Ikeda and K. Matsumoto, High-dimensional chaotic behavior in systems with time-delayed feedback, *Physica D*, **29**, (1987) 223-235.

[35] J. Farmer, Chaotic attractors of an infinite-dimensional dynamical system, *Physica D*, **4**, (1982) 366-393.

[36] J. Hale and S. Lunel, Introduction to functional differential equations, Springer-Verlag, New York, 1993.

[37] J.C. Sprott, A simple chaotic delay differential equation, *Phys. Lett. A*, **366**, (2007) 397-402.

[38] W. Tang, G. Zhong, G. Chen, and K. Man, Generation of n-scroll attractors via sine function, *IEEE Trans. Circuits Syst., I*, **48**, (2001) 1369-1372.

[39] X. Wang, G. Zhong, K. Tang, K. Man, and Z. Liu, Generating chaos in Chua's circuit via time-delay feedback, *IEEE Trans. Circuits Syst., I*, **48**, (2001) 1151-1156.

Received June 2010; revised October 2011.

email: journal@monotone.uwaterloo.ca
http://monotone.uwaterloo.ca/∼journal/